Evaluation of the potential of NASA multi-satellite precipitation analysis in global landslide hazard assessment

Yang Hong,[1,2] Robert Adler,[2] and George Huffman[2,3]

Received 13 September 2006; revised 18 October 2006; accepted 24 October 2006; published 28 November 2006.

[1] Intense storms with high-intensity, long-duration rainfall have great potential to trigger rapidly moving landslides, resulting in casualties and property damage across the world. In recent years, through the availability of remotely sensed datasets, it has become possible to conduct global-scale landslide hazard assessment. This paper evaluates the potential of the real-time NASA TRMM-based Multi-satellite Precipitation Analysis (TMPA) system to advance our understanding of, and predictive ability for, rainfall-triggered landslides. Early results show that the landslide occurrences are closely associated with the spatial patterns and temporal distribution of rainfall characteristics. Particularly, the number of landslide occurrences and the relative importance of rainfall in triggering landslides rely on the influence of rainfall attributes (e.g. rainfall climatology, antecedent rainfall accumulation, and intensity-duration of rainstorms). TMPA precipitation data are available in both real-time and post-real-time versions, which are useful to assess the location and timing of rainfall-triggered landslide hazards by monitoring landslide-prone areas while receiving heavy rainfall. For the purpose of identifying rainfall-triggered landslides, an empirical global rainfall intensity-duration threshold is developed by examining a number of landslide occurrences and their corresponding TMPA precipitation characteristics across the world. These early results, in combination with TRMM real-time precipitation estimation system, may form a starting point for developing an operational early warning system for rainfall-triggered landslides around the globe. **Citation:** Hong, Y., R. Adler, and G. Huffman (2006), Evaluation of the potential of NASA multi-satellite precipitation analysis in global landslide hazard assessment, *Geophys. Res. Lett.*, *33*, L22402, doi:10.1029/2006GL028010.

1. Introduction

[2] Landslides are one of the most widespread natural hazards [*Bryant*, 2005] and cause billions of dollars in damages and thousands of deaths and injuries each year around the world [*International Federation of Red Cross and Red Crescent Societies*, 2003]. Landslides occur in all U.S. states and territories, and they cause an estimated $2 billion in damages and 25–50 deaths every year in the U.S. (United States Geology Survey, United States Geology Survey landslide hazard, 2006, available at http://landslides.usgs.gov/). Thousands of landslides can be triggered by a single intense storm, causing spectacular damage in a short time over a wide area. The 1982–83 El Niño seasons triggered landslide events that affected the entire Western United States (including California, Washington, Utah, Nevada, and Idaho) and caused $400 million in losses in the Thistle, Utah, landslide, the most expensive single landslide in U.S. history [*Spiker and Gori*, 2003]. In Puerto Rico, rainfall-induced debris flows are by far the most abundant natural disaster [*Larsen and Simon*, 1993] and have resulted in substantial property damage and human life. For example, the Mameyes landslides triggered during a storm in October 1985 is considered one of the worst landslide disasters in U.S. history with 129 deaths [*Jibson*, 1989]. In December 1999, heavy rainstorms induced thousands of landslides along the Cordillera de la Costa, Vargas, Venezuela and fatalities were estimated to be at least 30,000 [*Larsen et al.*, 2000]. In 1998 a total of 9,871 landslides were triggered by Hurricane Mitch in Guatemala alone [*Bucknam et al.*, 2001].

[3] Landslides are a significant component of many major natural disasters and are responsible for greater losses than is generally recognized. Assessment of landslide hazards requires knowledge of the factors determining the probability of landslides, which according to *Dai et al.* [2002] can be grouped into two categories: (1) preparatory variables which make the land surface susceptible to failure (including topography, tectonics, geological history, weathering rates, land use, etc.) and (2) dynamic triggering factors (rainfall, earthquake, and glacier outburst). Landslides occurrence depends on complex interplay of many factors from the two categories. Remote sensing has been used in the detection and identification of diagnostic features mostly related to the first category, and to a lesser extent, to the detection of potential triggering factors as studied by *Kniveton et al.* [2000], *Buchroithner* [2002], *Huggel et al.* [2002], and *Kääb et al.* [2003]. Consequently, researchers have increasingly devoted attention to assessing the landslide triggering mechanism. In this study, we are primarily concerned with rainfall-triggered shallow landslides or debris flows. Hereafter we use the term landslides to refer to these types of landmass movement. For rainfall-induced landslides, the effect can occur in many forms such as snowmelt, change in ground-water levels, and water-level changes along coastlines, reservoirs, and riverbanks; however, extreme rainfall of high intensity and/or long duration is among the most common landslide-triggering mechanisms [*Dai et al.*, 2002].

[4] Rainfall-triggered land mass movements can be foreseen by examining the empirical relationship between rainfall characteristics and past landslide occurrence [*Keefer*

[1]Goddard Earth Science Technology Center, University of Maryland Baltimore County, Baltimore, Maryland, USA.

[2]Laboratory for Atmospheres, NASA Goddard Space Flight Center, Greenbelt, Maryland, USA.

[3]Science Systems and Applications, Inc., Lanham, Maryland, USA.

0094-8276/06/2006GL028010$05.00

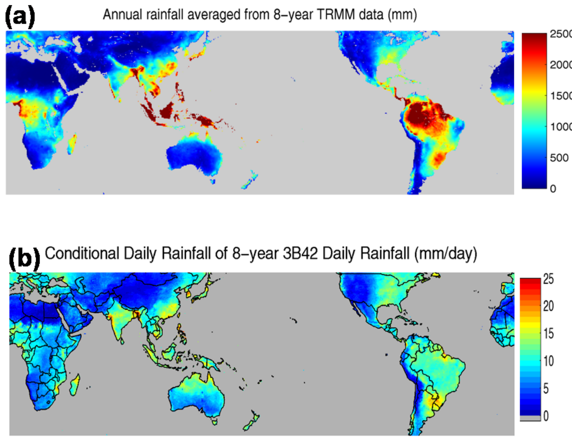

Figure 1. Rainfall climatology averaged from NASA 8-year (1998–2005) TRMM-based Multi-satellite Precipitation Analysis [*Huffman et al.*, 2006]: (a) annual mean of rainfall and (b) conditional daily rainfall.

et al., 1987]. Rainfall characteristics that lead to slope failure have been investigated both worldwide [*Caine*, 1980] and in specific regions, including Puerto Rico [*Larsen and Simon*, 1993], Hong Kong [*Finlay et al.*, 1997], Seattle [*Godt et al.*, 2006], and central and southern California [*Cannon*, 1988]. Although the characteristics of rainfall are critical to the initiation of slope failure, currently no system provides a real-time global overview of rainfall conditions that may trigger landslides. Such a system requires fine-scale precipitation information that is available continuously in time and space. Conventional ground monitoring networks for precipitation information are largely inadequate for this purpose, particularly in many developing countries due to insufficient hydrometeorological networks, long delays in data transmission, and the lack of data sharing in many trans-boundary river basins. As a result, sometimes altitude was used as an approximate surrogate for precipitation to help stratify landslide hazards because few regions with complex terrains have well-maintained precipitation monitoring network [*Sidle and Ochiai*, 2006]. The NASA TMPA precipitation product provides an opportunity to evaluate how rainfall attributes affect the spatial distribution and timing of landslides in regions that suffer from scarce *in situ* data.

[5] The goal of this paper is to evaluate the potential of the TMPA products to advance our ability to understand and predict rainfall-related landslides. Rainfall characteristics (e.g. annual mean; antecedent storm precipitation; and rainfall intensity-duration) strongly influence landslide occurrence [*Sidle and Ochiai*, 2006]. The space-borne satellite sensors capture complex spatial patterns in precipitation and provide frequent observations, and they can be used with regional slope-stability models that explicitly account for the transient effects of infiltration on the pore-pressure at depth [e.g., *Wu and Sidle*, 1995; *Iverson*, 2000; *Baum et al.*, 2002] to attempt to identify the spatial-temporal distribution of landslide initialization in complex terrains at real-time fashion. The availability of such information is critical to improving our predictive ability of rainfall-triggered landslides in areas where precipitation observations either do not exist at all or the deployed ground monitoring network has limited spatial coverage.

[6] Section 2 briefly describes NASA TRMM-based precipitation products, followed by evaluation of the TRMM multi-year products for landslide hazard assessment in Section 3. Section 4 provides concluding remarks.

2. Precipitation Observations From Space

[7] During the past twenty-five years information from a number of satellites has been compiled to give a better understanding of how precipitation is distributed across our planet. A continued development in the estimation of precipitation from space has culminated in sophisticated satellite instruments and techniques to combine information from multiple satellites to produce long-term products useful for weather and climate monitoring [*Adler et al.*, 2003]. The key data set used in this study is the TMPA [*Huffman et al.*, 2006], which provides a calibration-based sequential scheme for combining precipitation estimates from multiple satellites, as well as gauge analyses where feasible, at fine scales (0.25° × 0.25° 3-hourly) over the latitude band 50°N-S (http://trmm.gsfc.nasa.gov). The TMPA is a TRMM standard product that is being computed for the entire TRMM period (January 1998–present). It is available both in and after real time, based on calibration by the TRMM Microwave Imager and TRMM Combined Instrument precipitation products, respectively. Only the after-real-time product incorporates gauge data at the present, and this is implemented as a scaling between the 3-hourly satellite estimates and a monthly satellite-gauge combination. According to *Huffman et al.* [2006], at fine scales the TMPA is successful at approximately reproducing the surface-observation-based histogram of precipitation, as well as reasonably detecting large daily events. Examples are provided of a flood event and diurnal cycle determination. It is anticipated that the TRMM products will be succeeded by products developed for the Global Precipitation Measurement (GPM) mission (http://gpm.gsfc.nasa.gov). GPM is envisioned as providing fully global precipitation estimates (90°N-S) that combine all available satellite data, which is the goal of the TMPA.

3. Influence of TRMM Rainfall Characteristics on Landslides

3.1. Long-Term Precipitation: Annual and Seasonal Precipitation

[8] Rainfall-induced landslide occurrences are closely associated with spatial patterns of annual rainfall or seasonal rainfall [*Sidle and Ochiai*, 2006] and many other preparatory factors [*Dai et al.*, 2002]. Figure 1a shows the annual mean of precipitation averaged from the current 8-year TMPA dataset and masked to just show land areas. If a year's worth of global rainfall were spread evenly over the globe, the average depth of water would be waist deep, about one meter (908 mm). Over land, the average depth would be 791 mm per year. However, precipitation is not evenly distributed across our planet, but has striking spatial-temporal variations from place to place. Heavy annual rainfall occurs over the Maritime continent, Amazon basin, southeastern South America, Central America, western

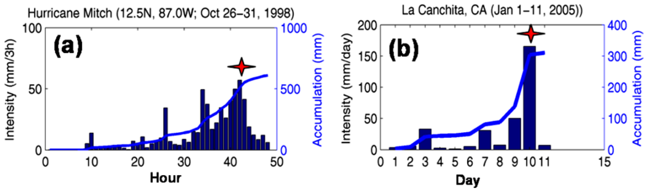

Figure 2. Influence of rainfall characteristics on the timing and occurrence of landslides. Bars are the rainfall intensity and star denotes the timing of landslide occurrence.

Pacific Rim, Himalayas Mountains and neighboring regions, and Congo basin. Figure 1b displays the conditional daily rainfall (rainfall amount averaged only over raining days) derived from the 8-year TMPA record, which clearly shows India, the rest of South Asia and East Asia, and many of the coastal areas along the margins of the Pacific Rim experience high annual rainfall with distinct conditional daily rainfall. Typhoons and monsoons, which often deliver both copious and intense rainfall, are common along the Asian continental and equatorial margins of the Pacific. For Central America the annual rainfall is between 1000 to 3000 mm but most of the rain falls during hurricane season from June to October.

[9] Scientists have generally thought that the rainfall must have certain amount necessary to saturate the landmass in hill slopes to a sufficient depth to cause a landslide. As a general rule, for example, a minimum of 250 mm of cumulative winter rainfall are needed to make Southern California hillsides susceptible to landslides; afterward, more than 50 mm (2 inches) in 6 hours in the lowlands or more than 100 mm (4 inches) in 6 hours in the mountains, can trigger landslides [*Campbell*, 1975; United States Geology Survey, Southern California landslides—An overview, 2005, available at http://pubs.usgs.gov/fs/2005/3107/pdf/FS-3107.pdf]. Similarly, the circum-Pacific region is naturally susceptible to landslides because of a combination of high and intense rainfall, mountainous terrain, and geological conditions [*Sidle and Ochiai*, 2006]. The high annual rainfall or heavy storms that affect India, Japan, China (including Hong Kong and Taiwan), Peru, Bangladesh, the West Coast of U.S., Appalachian Mountains, and Central America places them into the category of landslide-prone regions. As shown in Figure 1, the regions with high annual rainfall or high conditional daily rainfall (e.g. monsoon, hurricane season) cover the landslide-prone areas described by *Sidle and Ochiai* [2006].

3.2. Antecedent Precipitation Accumulation

[10] TMPA precipitation data are available both in real-time and archived after-real-time, which are useful for retrospectively investigating antecedent precipitation conditions. Particularly, in order to identify when landslide occurrences receive heavy rainfall, the operational TMPA rainfall can be accumulated at various space-time scales to examine the storm magnitude and antecedent precipitation. Figure 2 shows the influence of rainfall characteristics on the timing and occurrence of several landslides, which occurred during or just following periods of relatively substantial rainfalls.

[11] Figure 2a shows the TMPA rainfall intensity (bar) and accumulation (line) of one devastating landslide (>2500 deaths) that occurred at Casita Volcano, Nicaragua, on October 30, 1998. Following one week of heavy rainfall (>700 mm), the landslide swept over the towns of El Provenira and Rolando Rodriguez on October 30, 1998, the day of peak rainfall as Hurricane Mitch (then tropical storm) moved across Central America [*Scott et al.*, 2005]. Another example shown in Figure 2b: on January 10, 2005 at local time 1:20 pm, a massive debris flow swept through the coastal hamlet of La Conchita, California, and buried four blocks of the town, killing 10 people and destroying 50 homes. Figure 2b shows the antecedent 10-day rainfall intensity and accumulation.

3.3. Rainfall Intensity-Duration Threshold

[12] Evaluation of rainfall conditions that may trigger landslides has typically relied on empirical correlations of rainfall intensity and duration with landslide occurrences [e.g., *Caine*, 1980]. The relations between rainfall intensity and rainstorm duration often take the form of a power-law function [*Caine*, 1980; *Larsen and Simon*, 1993; *Godt et al.*, 2006]. Following their methods, an empirical landslide-triggering rainfall intensity-duration threshold can be derived by examining rainfall characteristics which triggered landslides in a variety of locations around world (including varying geologic and climatic characteristics). These rainfall-induced landslide cases were identified from news archives, reports, and websites, and then the corresponding rainfall intensity and duration information were computed from the TMPA database. Figure 3a shows the averaged rainfall intensity and storm duration for the 74 landslide events identified in the TRMM operational period (1998–present). These data were plotted on a double logarithmic scale, yielding the scattered distribution shown in Figure 3b. Despite the variations, it is clear that the production of these landslides requires intense rainfall,

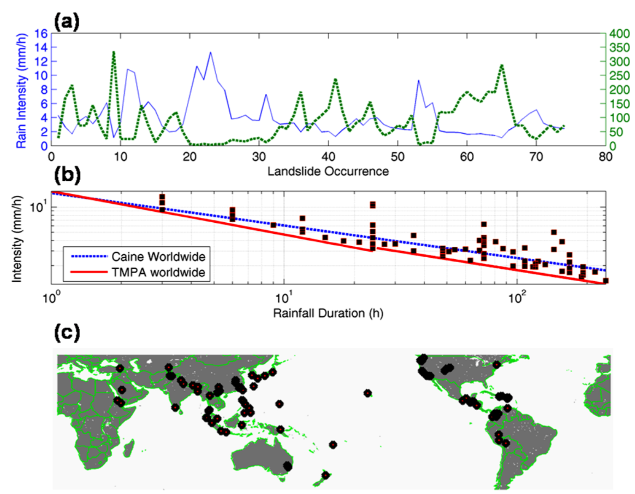

Figure 3. Rainfall intensity and duration of landslides occurring in TRMM operational period (1998–present). (a) Averaged rainfall intensity and duration of each occurrence; (b) lower bound of TMPA rainfall intensity-duration threshold (Intensity = 15.58 Duration −0.52 for sub-daily and Intensity = 13.35 Duration −0.44 for duration larger than 24 hours) for the landslide cases (squares) along with *Caine*'s [1980] global threshold; (c) the locations of the occurrences.

Table 1. Example of Destructive Rainfall-Triggered Landslides in the Past Eight Years[a]

Time	Place	Rainfall/Causes	Major Losses and Damage
07/14/2006	Hunterville, New Zealand	95mm/47 hours	Unknown
07/12/2006	Central Chile	183mm/70 hours	12 deaths
07/09/2006	South Korea	Typhoon Ewiniar, 300mm/70 hours	Widespread mudslide
07/07/2006	Wakayama, Japan	201mm/60 hours	Unknown
06/28/2006	Albany, upstate of NY	Heavy rainfall, 400mm/5 days	2 killed
04/13/2006	Buenaventura, Colombia	Rain storm, 103mm/1 day	>34 death
03/25/2006	Oahu, Hawaii	450mm/7 days	Tornado
03/21/2006	Papua New Guinea	44mm/1 day	Unknown
03/13/2006	Kukuryak, Bulgaria	74mm/18 hours	Unknown
02/17/2006	Guinsaugon, Southern Leyte, Philippines	Storm/earthquake, 685mm/14days	>1500 deaths
02/05/2006	Fiji	65mm/2 days	Unknown
01/04/2006	Jakarta, Indonesia	Monsoon rains, 250mm/3 days	>200 buried
10/8/2005	Solola, Guatemala	Hurricane Stan, 300mm/3 days	>1800 death
09/28/2005	Southern Mexico	150mm/3 days	3 deaths, thousands displaced
09/05/2005	Yuexi County, Anhui, China	Rain storm, 450mm/6 days	210,000 people affected; 10,000 houses flattened
08/07/2005	Southwestern Bulgaria	212mm/4 days	3 deaths
08/05/2005	Guwahati, India	Monsoon Rain, 310mm/3 days	5 killed
04/13/2005	Santa Cruz, CA	Storm, 147mm/1 day	2 deaths
03/09/2005	Cavallerizzo, Italy	29mm/3 hours	Unknown
03/07/2005	Southern Bulgaria	55mm/9 hours	Unknown
01/10/2005	La Conchita, CA	Heavy rain season, 390mm/14 days	12 deaths
11/13/2003	Puerto Rico	Hurricane, 145mm/1 day	Unknown
07/27/2003	Douglas County, Colorado	39mm/3 hours	Highway 67 closed
01/20/2003	Minamata and Hishikari, southern Kyushu, Japan	Heavy and intense rainfall Debris avalanches and debris flows	25 deaths; 7 homes destroyed; roads, power and hot spring lines damaged
05/11/2003	Southwest Guizhou Province, China	Heavy rainfall and road construction; road-related landslides	35 road workers killed and 2 buildings and road destroyed
04/20/2003	Kara Tarik, Kyrgyzstan	Rain-on-snow; large landslides in Soviet-era uranium mining area	38 deaths; 13 homes destroyed; potential pollution of a river
06/05/2001	Puerto Rico	77mm/1 day	Tropic storm
05/06/2000	Puerto Rico	258mm/2 days	Tropic storm
12/16/1999	North coast of Venezuela near Caracas	Nearly 900mm/3 days; Widespread shallow landslides and debris flows along a 40-km coastal strip	About 30,000 deaths; 8,000 residences and 700 apartments destroyed; extensive infrastructure damage
08/22/1999	Puerto Rico	255mm/3 days	Hurricane Debby
10/30/1998	Casita Volcano, Nicaragua	Hurricane Mitch, 720mm/6 days	>2000 death
09/22/1998	Puerto Rico	450mm/3 days	Hurricane
08/31/1998	Nishigo, Shirakawa, and Nasu, Japan	5 days of heavy rainfall	9 deaths; many homes/buildings destroyed
08/17/1998	Malpa, Northern India	4 days of heavy rainfall Large rockfall/debris avalanche	207 deaths; 5.2 million rupees direct cost and 0.5 million rupees indirect cost

[a]Collected from landslide inventory archives, with the addition of *Lagman et al.* [2006] and *Sidle and Ochiai* [2006]; the rainfall computed from NASA TRMM rainfall database.

sustained for at least a brief period of time. The rainfall intensity-duration (I-D) threshold triggering landslides was approximated by inspection to the lower boundary of the scattered data (squares) and the expressions are:

$$I = 15.58\ D^{-0.52}\ for\ D < 24\ hours \quad (1)$$

$$I = 13.35\ D^{-0.44}\ for\ D => 24\ hours \quad (2)$$

where I is the intensity in millimeters per hour, and D is the rainfall duration in hours. For comparison purpose, Figure 3b also displays the rainfall threshold obtained by *Caine* [1980] based on worldwide data (73 landslide occurrences). Figure 3c displays the minimum rainfall total (at different durations) needed to trigger landslides according to results of this study (e.g. Equation 1–2) and *Caine*'s [1980]. The new threshold proposed here falls below Caine's threshold and it is possibly due to the coarser scale of the TMPA. However, they are very close to each other at short-term duration less than 12 hours, which demonstrates that high-intense rainfall is necessary in order to trigger landslides. Note that one line, I = 12.45 $D^{-0.42}$, would be applicable for all rainfall duration if we don't allow a discontinuity at a duration of 24 hours (Figure 3b).

4. Discussion and Future Activities

[13] Landslides are a significant component of many major natural disasters and are responsible for greater losses than is generally recognized (Table 1). To predict the potential that specific regions might experience rainfall-induced landslides, some estimate of the rainfall conditions is needed. This paper evaluates the potential of the NASA TMPA precipitation estimation system in landslide hazard assessment. Early results show that the landslide occurrence is closely associated with the spatial patterns and temporal distribution of rainfall characteristics. Particularly, the num-

ber of landslides and the relative importance of rainfall in triggering landslides rely on the influence of rainfall attributes (e.g. rainfall climatology, antecedent rainfall accumulation, and intensity-duration of rainstorms). For the purpose of prediction, therefore, an empirical approach has been used to relate rainfall intensity and duration to landslides. The empirical Intensity-Duration threshold developed in this study using the TMPA real-time rainfall estimation system may form a starting point for developing an operational landslide monitoring/warning system across the globe. Real-time estimates of 3-hour precipitation from the TMPA will be compared with the intensity-duration thresholds; while antecedent rainfall accumulation can also be computed from the TMPA database. Therefore, the location and timing of any threshold exceedence can then be identified and checked against later news report. The results can be used to assess and modify the antecedent rainfall values and the empirical intensity-duration thresholds.

[14] Although the empirical rainfall intensity-duration thresholds have their limitations, they have been successfully implemented in several regions, including San Francisco Bay [*Keefer et al.*, 1987]; Rio de Janeiro, Brazil [*d'Orsi et al.*, 2004]; and Hong Kong [*Chan et al.*, 2003]. While such systems have proved very useful and may save lives and protect property, the requisite level of data collection, transmission, and warning is not yet practical in most vulnerable regions of developing countries that need it the most [*Sidle and Ochiai*, 2006]. The current NASA TRMM and future GPM systems offer an opportunity to develop/test a prediction system for landslides over large areas. However, more thorough evaluation of the potential of space-borne precipitation estimates in assessing rainfall-triggered landslides must await the development of such system. Future work includes applying the real-time TMPA rainfall estimates to deterministic slope-stability models [e.g., *Baum et al.*, 2002; *Dhakal and Sidle*, 2004] over broad regions to detect rainfall conditions that may lead to landslides. Two research directions are underway: (1) developing a global landslide susceptibility map by combing geospatial datasets, including elevation, slope, soil and geological properties, and land cover types, and (2) regionalizing the rainfall intensity-duration threshold according to various mean climatic variables (e.g. mean annual rainfall) to normalize the threshold values for different geographic regions and climate zones.

[15] **Acknowledgments.** This research is carried out with support from NASA's Applied Sciences program under Steven Ambrose of NASA headquarters.

References

Adler, R. F., et al. (2003), The version-2 Global Precipitation Climatology Project (GPCP) monthly precipitation analysis (1979–present), *J. Hydrometeorol.*, *4*, 1147–1167.

Baum, R. L., W. Z. Savage, and J. W Godt (2002), TRIGRS—A FORTRAN program for transient rainfall infiltration and grid-based regional slope-stability analysis, *U.S. Geol. Surv. Open File Rep. 02-0424*, 64 pp. (Available at http://pubs.usgs.gov/of/2002/ofr-02-424/.)

Bryant, E. (2005), *Natural Hazards*, 2nd ed., Cambridge Univ. Press, New York.

Buchroithner, M. (2002), Meteorological and Earth observation remote sensing data for mass movement preparedness, *Adv. Space Res.*, *29*(1), 5–16.

Bucknam, R. C., J. A. Coe, M. M. Chavarria, J. W. Godt, A. C. Tarr, L. Bradley, S. Rafferty, D. Hancock, R. L Dart, and M. L. Johnson (2001), Landslides triggered by Hurricane Mitch in Guatemala—Inventory and discussion, *U.S. Geol. Surv. Open File Rep. 01-0443*.

Caine, N. (1980), The rainfall intensity-duration control of shallow landslides and debris flows, *Geogr. Ann.*, *62A*, 23–27.

Campbell, R. H. (1975), Soil slips, debris flows and rainstorms in the Santa Monica Mountains and vicinity, southern California, *U.S. Geol. Surv. Prof. Pap. 851*.

Cannon, S. H. (1988), Regional rainfall-threshold conditions for abundant debris-flow activity, in *Landslides, Floods, and Marine Effects of the Storm of January 3–5, 1982, in the San Francisco Bay Region, California*, edited by S. D. Ellen and G. F. Wieczorek, *U.S. Geol. Surv. Prof. Pap. 1434*, 35–42.

Chan, R. K. S., P. L. R. Pang, and W. K. Pun (2003), Recent developments in the landslip warning system in Hong Kong, in *Geotechnical Engineering—Meeting Society's Needs, Proceedings of the 14th Southeast Asian Geotechnical Conference*, edited by K. K. S. Ho and K. S. Li, pp. 219–224, A. A. Balkema, Brookfield, Vt.

Dai, E. C., C. F. Lee, and Y. Y. Nagi (2002), Landslide risk assessment and management: An overview, *Eng. Geol.*, *64*, 65–87.

Dhakal, A. S., and R. C. Sidle (2004), Distributed simulations of landslides for different rainfall conditions, *Hydrol. Processes*, *18*, 757–776.

d'Orsi, R. N., R. L. Feijo, and N. M. Paes (2004), 2,500 operational days of Alerta Rio System: History and technical improvements of Rio de Janeiro Warning System for severe weather, in *Landslides: Evaluation and Stabilization*, edited by W. A. Lacerda et al., pp. 831–842, Taylor and Francis, Philadelphia. Pa.

Finlay, P. J., R. Fell, and P. K. Maguire (1997), The relationship between the probability of landslide occurrence and rainfall, *Can. Geotech. J.*, *34*, 811–824.

Godt, J. W., R. L. Baum, and A. F. Chleborad (2006), Rainfall characteristics for shallow landsliding in Seattle, Washington, USA, *Earth Surf. Processes Landforms*, *31*, 97–110.

Huffman, G. J., R. F. Adler, D. T. Bolvin, G. Gu, E. J. Nelkin, K. P. Bowman, Y. Hong, E. F. Stocker, and D. B. Wolff (2006), The TRMM Multi-satellite precipitation analysis: Quasi-global, multi-year, combined-sensor precipitation estimates at fine scale, *J. Hydrometeorol.*, in press.

Huggel, C., A. Kääb, W. Haeberli, P. Teysseire, and F. Paul (2002), Remote sensing based assessment of hazards from glacier lake outbursts: A case study in the Swiss Alps, *Can. Geotech. J.*, *39*, 316–330.

International Federation of Red Cross and Red Crescent Societies (2003), World disasters report, 2003, 239 pp., Geneva, Switzerland.

Iverson, R. M. (2000), Landslide triggering by rain infiltration, *Water Resour. Res.*, *36*, 1897–1910.

Jibson, R. W. (1989), Debris flows in southern Puerto Rico, in *Proceedings: Landslide Processes of Eastern United States and Puerto Rico*, edited by A. P. Schulta and R. W. Jibson, *Spec. Pap. Geol. Soc. Am.*, *236*, 29–55.

Kääb, A., R. Wessels, W. Haeberli, C. Huggel, J. S. Kargel, and S. J. S. Khalsa (2003), Rapid ASTER imaging facilitates timely assessment of glacier hazards and disasters, *Eos Trans. AGU*, *84*(13), 117.

Keefer, D. K., et al. (1987), Real-time landslide warning during heavy rainfall, *Science*, *238*, 921–925.

Kniveton, D., P. de Graff, K. Granicas, and R. Hardy (2000), The development of a remote sensing based technique to predict debris flow triggering conditions in the French Alps, *Int. J. Remote Sens.*, *21*(3), 419–434.

Lagmay, A. M. A., et al. (2006), Scientists investigate recent Philippine landslide, *Eos Trans. AGU*, *87*(12), 121.

Larsen, M. C., and A. Simon (1993), A rainfall intensity-duration threshold for landslides in a humid-tropical environment, Puerto Rico, *Geogr. Ann.*, *75A*, 13–23.

Larsen, M. C., G. F. Wieczorek, L. S. Eaton, H. Torres-Sierra, and B. A. Morgan (2000), The December 1999 rainfall-triggered landslide and flash-flood disaster in Vargas, Venezuela, *Eos Trans. AGU*, *81*(48), Fall Meet. Suppl., Abstract H12B-02.

Scott, K. M., J. W. Vallance, N. Kerle, J. L. Macías, W. Strauch, and G. Devoli (2005), Catastrophic precipitation-triggered lahar at Casita Volcano, Nicaragua: Occurrence, bulking, and transformation, *Earth Surf. Processes Landforms*, *30*, 59–79.

Sidle, R. C., and H. Ochiai (Eds.) (2006), *Landslides: Processes, Prediction, and Land Use*, *Water Resour. Monogr.*, vol. 18, AGU, Washington, D. C.

Spiker, E. C., and P. L. Gori (2003), National landslide hazards mitigation strategy—A framework for loss reduction, *U.S. Geol. Surv. Circ. 1244*, 1–64.

Wu, W., and R. C. Sidle (1995), A distributed slope stability model for steep forested basins, *Water Resour. Res.*, *31*, 2097–2110.

R. Adler, Y. Hong, and G. Huffman, NASA Goddard Space Flight Center, Mail code 613.1, Greenbelt, MD 20771, USA. (yanghong@agnes.gsfc.nasa.gov)